Theoretical Background and Prognostic Modeling for Benchmarking SHM Sensors for Composite Structures

Vadim Smelyanski[1], Vasyl Hafiychuk[1], Dmitry G. Luchinsky[1],

Curtis Banks[2], Chris Conn[2], Jim Miller[2], Mike Watson[2]

[1] *NASA Ames Research Center, Mail Stop 269-2, Moffett Field, CA 94035, USA*
Vadim.N.Smelyanskiy@nasa.gov Vasyl.Hafiychuk@nasa.gov
Dmitry.G.Luchinsky@nasa.gov

[2] *NASA Marshall Space Flight Center, Huntsville, Al 35812 USA*
Curtis.E.Banks@nasa.gov Chris.Conn@nasa.gov
Jim.Miller@nasa.gov Mike.Watson@nasa.gov

ABSTRACT

This paper reports on analytical as well as computer simulation of waves propagating in sandwich-type composite structures. Sandwich-type composites are being studied for use in NASA's new heavy lift launch vehicle, and flaw detection is crucial for safety and for failure prognostics. Theoretical analysis, as well as numerical modeling, is needed for benchmarking of available technologies for structural health monitoring (SHM) sensors and sensor systems. This benchmarking activity is important for answering the basic question of what minimum flaw size can be detected by the existing SHM based monitoring methods.

Sandwich panels with foam, WebCore and honeycomb structures were considered for use in this study. Eigenmode frequency analysis and Frequency Response Analysis of the panels were made to understand fundamental properties of the panel physics and limitations that may affect the application of current SHM sensors and methods. An analytical study of the transient wave propagation is considered based on Mindlin plate theory. The mathematical model, accompanied by numerical simulations, shows that small size defects can be recognized but the frequency of waves should be sufficiently high. It is concluded that a combination of analytical results coupled with the high-fidelity simulations should make it possible to analyze experimental data and to predict the applicability of SHM methods for this type of structure. [*]

1. INTRODUCTION

As the size and complexity of space hardware grows, structural weight control becomes crucial. This is the case for NASA's new heavy lift launch vehicle. Weight control usually involves the use of lighter weight structures such as composites. Whether it be hat stiffened, corrugated sandwich, honeycomb sandwich, or foam filled sandwich, all composite structures have one basic handicap in common: they all share a failure mechanism that is so insidious as to make it difficult to impossible to discern when and where a serious flaw may occur. The reason is that structural failures will occur internally, out of view of normal visual means of inspection. Internal de-bonds, de-laminations, cracks, and/or buckles are typical failure modes. For faults such as these, which may be caused during fabrication, a normal non-destructive inspection technique (NDE) such as X-Ray, Thermography, or Sherography is useful, although very labor intensive.

For heavily loaded composites, such as the heavy lift launcher will undoubtedly employ, this type of damage represents a major safety concern, especially for man rated vehicles. Therefore the application of structural health monitoring (SHM) is an important consideration. For this purpose, several types of SHM sensors and application techniques have been developed and are finding wide spread use in commercial structures as well as aerospace systems. The prognostics associated with SHM involve modeling of the structure/sensor combination and running simulations that assume different levels of strain and vibration loads. To prognosticate the specific type and location of a

potential, critical failure mechanism is the name of the game. To this end, the advanced composite technology (ACT) program of NASA has put in place a team to evaluate the state of the art of SHM and to make recommendations to the heavy lift launch program. NASA's ACT Project is evaluating the performance of many different sensors and sensor systems for heavy lift vehicle (HLV) bulky structures: the Payload Shroud, the Interstage, the Core Intertank, the Storage Fuel Tank, the Crew Composite Modulus, and so forth. Some of the peculiarities of these structures be found in reports (e.g., B. Bednarcyk, et al., 2007), (B. Bednarcyk, et al., 2010), (D. W. Sleight et al., 2008).

These papers discuss one of the many tasks associated with development and benchmarking of SHM methods and provides an estimate and conclusions about the application of SHM in the domain of highly loaded composite structures. The use of a WebCore test panel is now being subjected to structurally damaging tests at MSFC. This paper presents the results of an analytical estimation and modeling of wave propagation in the WebCore sandwich along with the development of the mathematical model. It also compares the model predictions with the SHM sensors' empirical findings.

The bulky HLV structures are estimated to be 33 feet in diameter at the base. From the modeling point of view such large area structures could be considered as infinite, so the approach was developed for an infinite plate. This analytical approach makes it possible to predict acoustic fields in such composite structures with the view of using them in SHM. This paper focuses on simulation of

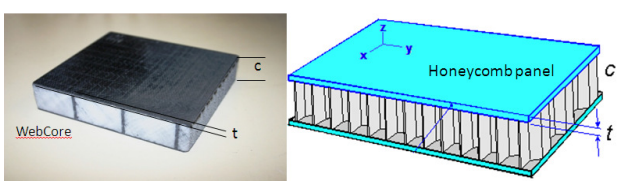

Figure 1: Sketch of the typical sandwich panel.

transient waves in the composite structure using the framework of Mindlin shell theory. The matter is that for developing SHM of large composite panels we need to have some analytical approach that makes it possible to play with parameters to optimize the detected procedure. Such an analytical approach is developed here based on 2D plate theory. Finite element (FE) 3D modeling of large panels is not always able to be done and use it for fault prediction. Therefore, combining analytical estimation with FE modeling is needed to deepen our understanding of how faults could be reliably detected. The modeling presented here is for the 1" thick panel manufactured for the express purpose of the SHM sensor benchmarking. We combined analytical approach with FE modeling to see where the simplified theoretical approach works. This type of model was needed to derive benchmark metrics.

Experiments in benchmarking sensors were performed and experimental data will be analyzed letter on. It should be noted that prior to specific modeling and empirical data generation, the panel was evaluated by standard NDE techniques that determined initial conditions identified and located any intrinsic flaws. An initial objective of SHM sensor benchmarking was to detect a small 1/4" diameter hole and to rank PZT and FBG sensor types according to their ability to detect such a flaw. Other criteria used in the benchmarking rank were the accuracy of hole location and the repeatability of the observation. Therefore, the models of damage studied here involved the scattering of flexural waves by a 1/4" hole drilled near the center of the panel.

Sandwich panels, to which we restrict our consideration here, are complex structural materials made from hard facesheets and soft cores and are usually referred to as sandwiches with soft cores. Soft-core (e.g., foam, WebCore, and honeycomb) sandwich structures' dynamic behaviors are characterized by two different scales: one is described by classical theories for sandwich panels, which is valid for scales greater than the sandwich thickness (shell theories approximation), and the second scale emerges when studying local vibrations inside soft cores on scales of the sandwich thickness.

The following section of the paper discusses sandwich panel parameters, the governing equations, and the properties of the sandwich panels. These were obtained from mathematical simulations based on FE modeling. The third section of the paper presents the solutions obtained and the analysis of the framework of the theory. A mathematical model of simple flow is considered, as well as transient wave generation and wave packet propagation. High-fidelity simulations are employed to compare results of simulations with analytical results.

2. SANDWICH PANEL PARAMETERS AND MODELING

2.1 Sandwich macroscopic characteristics

A typical geometry of the sandwich composite panel is sketched in Figure 1. For modeling reasons, the size of the panel is 1.2m x 1.2m. Approximate parameters of the sandwich panel layers are given in Table 1, where E_x (E_y,E_y) is the Young modulus in $x(y,z)$ direction, ρ is the density of the layer, G_{xy} (G_{xz},G_{yz}) is the shear modulus, and ν is a Poisson ratio. The exact parameters of the specific panels you can find in many books (See, for example,

Zenkert, 1997) as well as in manufacturer specifications. These parameters (Table 1) were taken for computer simulation, estimation of the macroscopic shell properties, and determination of the sandwich behavior under local load. For computer simulation, we considered a hole located at the center of the plate to minimize boundary influence on the scattering procedure.

Table 1. Characteristic parameters (by an order of magnitude) of the materials used for estimation

	$E_x(E_y,E_y)$ GPa	ρ, kg /m^3	$G_{xy}(G_{xz},G_{yz})$ GPa	ν
E-TLX330	~10	~1000	~5	~0.3
PVC Foam	~0.04	~60	~0.02	~0.2
TYCOR	~0.2	~300	~0.02	~0.3
CFRP	~100	~1500	~4	~0.3
Honeycomb	~0.7	~100	~0.4	0

Let us determine four structural parameters of the sandwich panel (Zenkert, 1997) starting from flexural rigidity D:

$$D = \frac{E_f t^3}{6} + \frac{E_c c^3}{12} + \frac{E_f t(t+c)^2}{2} = 2D_f + D_c + D_0, \qquad (1)$$

where E_f and E_c are Young module for face sheets and core, respectively, and t and c are the thicknesses of the sheets and core as shown in Figure 1. In this case, the sandwich plate has a thickness $h = 2t + c$. Each term in the right hand side is denoted by its own capital letter D.

Table 2. Values of characteristic parameters (by an order of magnitude) of the structures

Sandwich Panel	D, $N{\cdot}m$ $\times 10^4$	ρ, kg/m^2	G, $MPa{\cdot}m$	I, kg $\times 10^{-4}$
WebCore	1	5	1	5
Honeycomb	10	10	5	5

In the thin face sheet and weak core approximation, we have

$$D = E_f t(t+c)^2 / 2.$$

The shear stiffness of the sandwich panel in the same limit will be

$$G = G_c (c+t)^2 / c. \qquad (2)$$

The surface density of the panel is

$$\rho = 2\rho_f t + \rho_c c, \qquad (3)$$

and the symmetrical sandwich panel rotatory inertia is

$$I = \rho_f \frac{t^3}{6} + \rho_f \frac{t(t+c)^2}{2} + \frac{\rho_c c^3}{12}. \qquad (4)$$

Expressions (4) and (1) are the same except E_f and E_c are substituted by ρ_f and ρ_c, respectively. In Table 2 you can find the order of magnitude for the parameters of the sandwich structure calculated above. It should be noted that WebCore panel parameters in table 2 are the same as calculated for a foam core structure.

2.2 Mindlin Plate Theory

Parameters (1) - (4) are widely used for quasistatic modeling. These parameters can also be used for study of wave propagation. For the low frequency region (upper bound limit is determined by the plate parameters), this approach can be used for investigation of flexural waves (Rose & Wang, 2004). Mindlin plate theory is known to be sufficiently accurate to wavelengths comparable with the plate thickness, whereas classical plate theory is of acceptable accuracy only for wavelengths much greater than the plate thickness. Thus, Mindlin plate theory offers the prospect of good resolution of damage size, relative to classical plate, whereas an analysis using the exact 3D-elasticity equations would be quite intractable and could be realized only by direct computer simulation. That means Mindlin approach can be used as starting point for SHM modeling of the sandwich composite structures.

The displacements of a Mindlin plate are

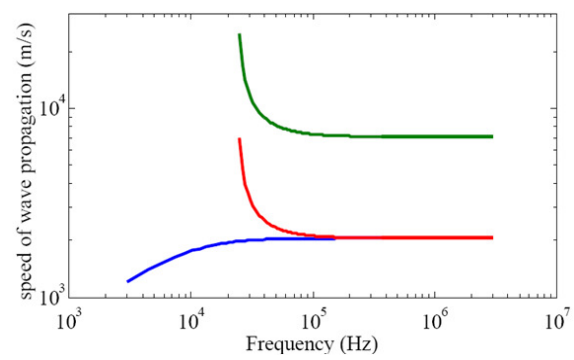

Figure 2: Typical dependencies of speed of wave propagation for sandwich panels.

expressed as (Mindlin, 1951)

$$u_x = \psi_x(x,y),\ u_y = \psi_y(x,y),\ u_z = w(x,y), \qquad (5)$$

where w is the transverse displacement of the mid-plane and ψ_x and ψ_y are the rotations of vertical lines perpendicular to the mid-plane. For the sake of simplicity we consider isotropic properties of the face-sheet and core materials with corresponding Young module and similar Poisson ratios. As a result, variables w, ψ_x and ψ_y satisfy the governing equations for the averaged values of sandwich parameters D, G, ρ, I and coincide of with equations for simple plate (Rose & Wang, 2004), (Mindlin, 1951):

$$\frac{D}{2}\left[(1-\nu)\Delta\boldsymbol{\psi}+(1+\nu)\nabla\nabla\boldsymbol{\psi}\right]-G(\boldsymbol{\psi}+\nabla w)=I\frac{\partial^2\boldsymbol{\psi}}{\partial t^2},$$

$$G(\Delta w+\nabla\boldsymbol{\psi})=\rho\frac{\partial^2 w}{\partial t^2}, \qquad (6)$$

where ν is a Poisson ratio and $\boldsymbol{\psi} = (\psi_x, \psi_y)$.

In one dimension, w, ψ_x, $\psi_y \sim \exp(ikx - i\omega t)$ and we have a system of three algebraic equations. Solvability of it gives a dispersion relation. In the one-dimensional case we

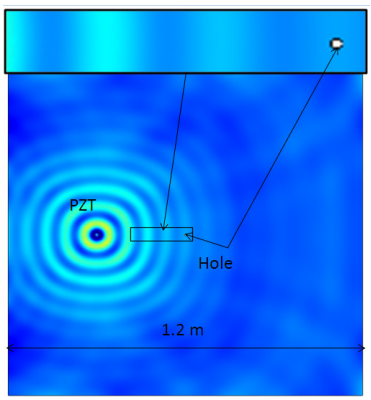

Figure 3: Finite element simulation of sandwich webcore structure used for benchmarking (1.2m x 1.2m). PZT actuator generates flexural waves with frequency f = 50 kHz. The hole area is zoomed out to show geometric scale (on the top plot).

have two main branches that are described by the expression (Thompson et al. 1975)

$$\omega^2 = b \pm \sqrt{b^2 - c},$$

where

$$b=\frac{1}{2}\left(\frac{G}{\rho}+\frac{D}{I}\right)k^2+\frac{1}{2}\frac{G}{I}, c=4GDk^4 \qquad (7)$$

Dispersion curves (Figure 2) for typical sandwich panels describe flexural waves (blue curve) corresponding to real ω and k and two branches of the ω,k relation that become real starting from the cut-off frequency (red and green curves).

The speed of flexural wave propagation in WebCore like structure is lower than in honeycomb structure. From the speed we can easily calculate the frequency required in order to have a wavelength comparable to the size of the hole: $f = c/\lambda \sim 10^3/6\cdot10^{-3}\ s^{-1} \sim 150$kHz. Such a frequency for thick sandwich structure, particularly WebCore structure, is too hard to realize in real structures due to attenuation and stimulation of large numbers of local modes, which lead to dissipation of energy. To clarify this statement, let us start with finite element simulation.

2.3 Finite element simulation

For benchmarking sensors, large panels were used to find out which sensors are capable of detecting such flow size at the maximum distance from the hole. A general sketch of computer simulation of the large WebCore (1.2m x 1.2m) panel is presented in Figure 3. You can see that for such a small hole no visual scattering can be observed. The simulations are made in Mindlin plate theory approach and averaged structural parameters correspond to WebCore of Table 2.

To understand acoustic wave propagation

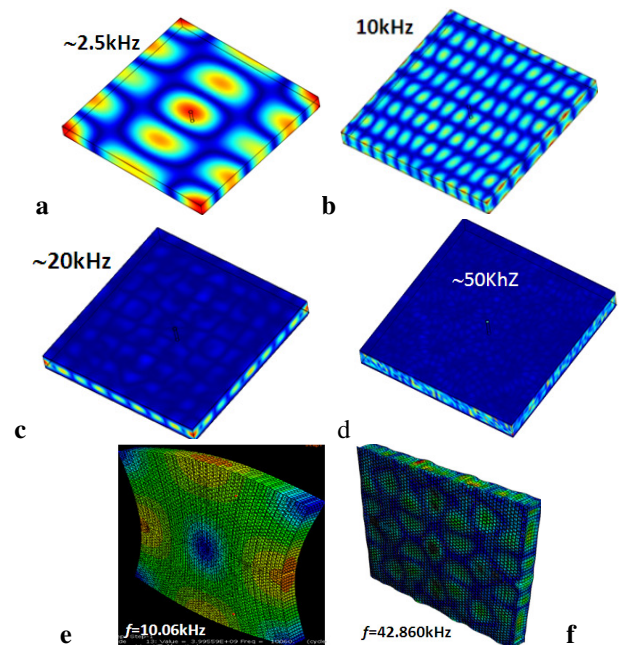

Figure 4: Shapes of eigenmodes for foam core panel – *a-c*, and honecomb sandwich panel – *e,f.* At higher frequencies ($f \geq 10$ kHz, for foam core and 30 kHz honeycomb panel), practically all normal modes are localized in the core, and facesheets practically do not respond.

through the 3D sandwich panel, eigenfrequencies and eigenfunctions were calculated for a smaller panel (0.3m x 0.3m) with 1in core thickness, 2mm facesheets, and a hole at the center (Figure 4). We considered three different structures: foam core sandwich panel, WebCore panel and honeycomb sandwich panel. From the theoretical point of view consideration of different panels is practically identical, just values of the parameters are different (Table 2). Finite element modeling takes into account intrinsic structure of the core and therefore is much more precise in modeling acoustic waves needed for SHM.

We started with investigation of the shapes of

the modes in each panel mentioned above. Some of the results for the foam core sandwich panel are presented in Fig. 4. We revealed that at relatively low frequencies (< 3kHz), the sandwich structure vibrates as a whole with around 30 different modes (Fig. 4a). The average separation for the modes is approximately 100Hz for this size of panel. Around 10 kHz, some of the modes are only realized in the core. By sweeping the sample for higher eigenmodes, we revealed that the spectrum becomes quasicontinuous and the majority of eigenmodes are located in the sandwich core. This trend is much more pronounced for eigenfrequencies ~ 50kHz, at which point practically all modes are localized in the core between facesheets (Fig. 4 c,d).

This phenomenon is due to the fact that the foam core sandwich panel and WebCore panels have a core with a much lower Young modulus than the facesheets, and as a result, a large number of local modes are realized in the structure without stimulated facesheet vibration. It should

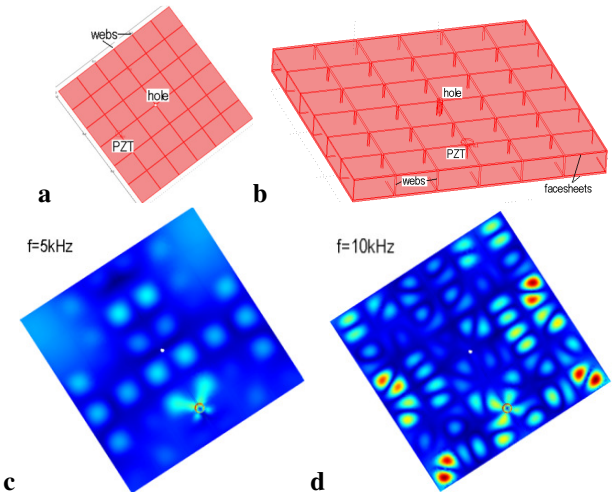

Figure 5: Finite Element model of the WebCore panel built in Comsol a), and b). Frequency response analysis pattern at f = 5kHz - c), and f = 10kHz - d).

be noted that webs between facesheets determine the shape of eigenmodes for only certain frequencies. The majority of the modes are determined by the core inside the cells, which are separated by webs. These modes at high frequencies will lead to damping, decreasing SHM options. In this case, we can state that macroscopic sandwich shell approximation is reasonable because it makes it possible to model the propagating wave stress strain distribution in WebCore, not taking into account the huge number of local modes that make SHM more difficult to realize. These local modes can be considered as an averaged field that determines attenuation for perturbation with the wavelength at least comparable to the thickness.

The same situation takes place in Honecomb panels. From Figure 4e you can see that facesheets and core vibrate as a whole similar to shell structure and we do not see any intrinsic oscillations inside honeycomb core. At higher frequency oscillations are mainly localized inside soft hexagonal structure of Aluminum core (Fig. 4f).

We performed frequency response analysis of the panels. The result of 3D FE simulation of one of the panels is presented in Figure 5. The first two plots explain the geometry of the panel and how it is used for FE simulation. The two others are stationary responses of the WebCore panel for PZT excitation. Total displacement patterns on Figure 5c show that at low frequency (5kHz) we see pronounced spatial distribution along the plate modulated by the webs' localization. Increase of the frequency leads to formation of the pattern shape with greater wave number. Due to sufficient difference in Young's modulus of the core and the webs', structural dynamics depends strongly on webs disdribution. We can see that even at low frequencies (5-10kHz) when the wavenumber is small Eigenmodes are modulated by the webs' localization. These results are simulated without damping but taking into account damping just decreases the amplitude of the patterns. This can be seen from the Figure 6.

The sandwich structure with foam core (without webs) was simulated for different frequencies (from 10Hz to 100kHz) to understand what frequency can be used for SHM. Figure 6 presents as an example the total displacement field, for a frequency of 17.5kHz, without damping (left) and with damping (right). You can see the change in the spatial structure of the modes as well as in the amplitudes of the displacement, which decrease significantly and thus are an additional limiting factor in SHM of WebCore panels. Such mode behavior in real structures can lead to dissipation and to limitation of wave propagation in the structures. One can find some attenuation data in the case of honeycomb structure, but there is practically no information on viscoelastic properties of sandwich panels in the case of a WebCore panel.

Evidently the Mindlin plate theory approach considers waves that are determined by plate vibration as a whole and does not take into account intrinsic complex structure and local modes of the panel.

The pronounced scattering pattern can be seen only for small distances (e.g. 10cm) from the sensor at high frequencies greater than 150kHz. Taking into account intrinsic inhomogeneities and large attenuation at high frequencies, we can state that SHM monitoring of WebCore and honeycomb panels is a challenge. The main factor that determines limitation of the SHM method is a structural noise, which is comparable to a scattered signal. This means that in order to have a high probability of detection (close to 100% for ¼ in), we have to have dense sensor location.

3. ANALYTICAL SOLUTION

Computer simulation of the 3D WebCore panel discussed above and the honeycomb structure panel made earlier show that shell approximation is good enough for long wavelengths. This section is devoted to the analytical solution and the major steps in developing this approach. First we consider stationary acoustics generated by a cylindrical source. Second, we solve the scattering problem in the stationary field, and finally, a transient wave packet is considered. These three steps make it possible to find an analytical solution in the Mindlin approach and use it in plate simulation.

3.1 Source term of the cylindrical waves

We will consider a circular-patch actuator on a Mindlin plate generating, via surface traction, plate waves in the form (Wang, Rose, & F.K. Chang, 2004):

$$w(r,\omega) = \frac{i\pi h p(\omega)}{4D} \frac{k_1 r_0 J_1(k_1 r_0) H_0(k_1 r)}{k_1^2 - k_2^2}, \tag{8}$$

where J_n and H_n are the Bessel and Hankel functions of the first kind, respectively, r_0 is the radius of the PZT actuator, and $p(\omega)$ is the source function of frequency, $\omega = 2\pi f$. The Hankel function H_0 in the expression is the only function depending on radius vector r, and it can be represented as the series expansion (Morse & Feshbach, 1953)

$$H_0(kr) = \sum_{n=0}^{\infty} \varepsilon_n (-1)^n H_n^1(kb) J_n(kr) \cos(n\theta), \text{for } r < b,$$

$$H_0(kr) = \sum_{n=0}^{\infty} \varepsilon_n (-1)^n H_n^1(kr) J_n(kb) \cos(n\theta), \text{for } r > b, \tag{9}$$

where ε_n is the Neumann factor ($\varepsilon_0 = 1$, $\varepsilon_n = 2$, $n = 1,2,3...$), b is the distance from the source to the hole, and k is the wavenumber equal to k_1 or k_2. Substituting Eq. (9) into Eq. (8), we get incident cylindrical waves represented by the series expansion.

3.2 Cylindrical hole scatterer

For theoretical investigation, we will consider that the circular hole distant from the source is located at the infinite plate. In this case, parameters of the plate outside the scatterer are determined by elastic properties of the medium, and the complete solution will be the sum of the propagations from the source signal and the scattered one. There are several models of the scatterers (Wang & F.K. Chang, 2005), but we limit our consideration here to the simplest one.

Following the work of Pao & Chao, 1964, the boundary conditions can be fulfilled as an average over the plate thickness with

$$M_{rr} = M_{r\theta} = Q_r = 0,$$

which are considered at $r = a$, and

$$w = \sum_{n=0}^{\infty} \{\varepsilon_n (-1)^n H_n(k_1 b) J_n(k_1 r) + a_{1n} H_n(k_1 r) + a_{2n} H_n(k_2 r)\} \cos(n\theta) \tag{10}$$

where Hankel functions H_n of the first kind determine the influence of wavenumbers k_i on the scattered field. The boundary conditions lead to a system of three linear algebraic equations for each value of n. These systems of equations relative to constants a_{1n} and a_{2n} can be solved numerically. It is

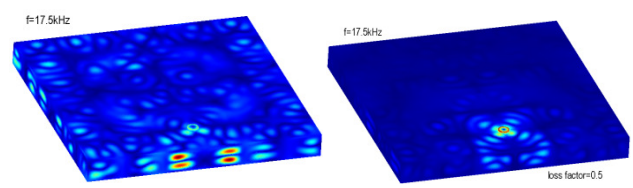

Figure 6: Stationary pattern of the total displacement of the WebCore panel at PZT frequency f=17.5kHz. The hole size ¼ in is located at the center and PZT on a distance 10cm from the hole. Right plot is simulated for the same parameters but for 0.5 core loss factor.

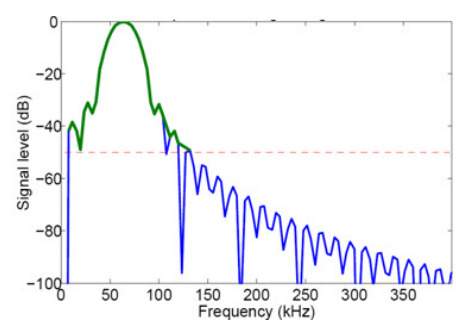

Figure 7: Spectrum G(ω) of the original signal (11) for f=60kHz

found that the truncations of n at n = 50 in Eq. (10) give the same result at any desired wave frequencies.

3.3 Transient Dynamics

The expression for the transverse wave pulses in the x,y -plane may be derived from the steady-state solution of the

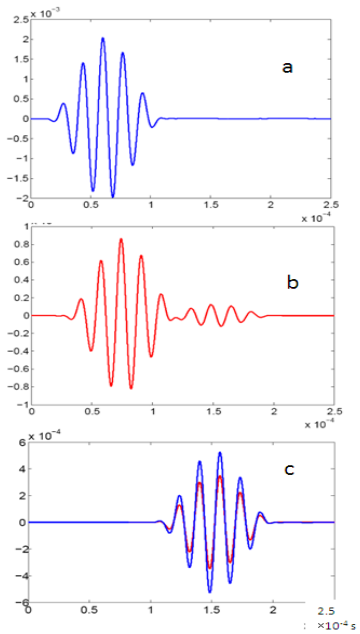

Figure 7: Analytical results of the real transverse displacement simulated by Matlab (Honeycomb panel parameters are implemented).

scatterer in the frequency domain by applying the Fourier transform technique. Any pulse of flexural waves can be expanded in the Fourier transform, which represents the pulse as a series of the flat waves. We used Hanning Windowed signal:

$$g(t) = \left[H(t) - H(t - \frac{2\pi N}{\omega}) \right] \left(1 - \cos\frac{\omega t}{N} \right) \sin(\omega t) \tag{11}$$

where N is a parameter of the pulse, $H(t)$ is a Heaviside function. The Fourier spectrum of this signal will be

$$g(t) = \frac{1}{2\pi} \int_{-\infty}^{\infty} G(\omega) e^{-i\omega t} d\omega ,$$

where $G(\omega)$ is the frequency spectrum of the input signal. The analytical solution of the Mindlin wave propagation and scattering is given by

$$w(t, r, \theta) = \frac{1}{2\pi} \int_{-\infty}^{\infty} G(\omega) w(\omega, r, \theta) e^{-i\omega t} d\omega \tag{12}$$

As a result, we have a distribution of the mechanical parameters in 2D plate. This solution can be used for estimation stress-strain fields under any sensor mounted to the plate.

3.4 Solution of the Mindlin wave propagation, scattering, and simulation

Solution of the transient dynamics is presented in Figure 8 for transverse displacement for different locations on the line connecting the PZT actuator with the hole. Figure 8a corresponds to input signal, Figure 8b to Pulsed echo signal, and Figure 8c to pitch-catch technique. We can see in Figure 8c that the left pulsed signal corresponds to a pristine signal and similar second small amplitude pulse to a signal reflected from the hole. In Figure 8c the pristine signal is blue and the red one is the theoretical signal calculated by taking into account scattering from the hole. We can conclude that those reflected and scattered signals are pronounced when the source term and a hole are located sufficiently close to each other. At large distances, the computer simulation errors make it impossible to distinguish between the baseline signal and the damaged one.

The obtained results show that analytical formulas expressed in Matlab simulation grasp the main characteristic features of the SHM methods and that such modeling is a viable and reasonable approach for predication of acoustic field propagating and scattering in structures in large-scale structure systems.

Finite element modeling of these structures makes it possible to compare 3D waves with the results obtained analytically. These simulations show that at the initial stage signals coincide, but when the generated signal reaches the boundaries these signals are quite different. The difference is caused by reflection of waves from the boundaries

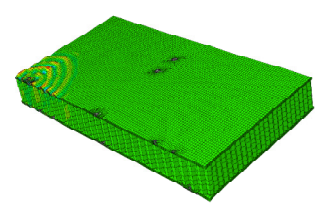

Figure 9: FE simulation of real honeycomb structure

arising in FE simulation of finite size structures. In the theoretical approach we consider infinite structure where waves do not have any boundaries.

For sandwich honeycomb structure, a finite element model was developed that takes into account all characteristic features of the panel: honeycomb periodic cells, interface layer, and laminate structure of facesheets (Figure 9). The first such modeling was made by Song, Huang, & Hudson, 2009. Main analyses are performed in the time domain in ABAQUS/Explicit for investigation of the signal propagation in the structure. The frequency range of interest was between 10 and 100

kHz. The signal that was taken as Hanning windowed was generated by the PZT sensor mounted on the surface. The form of the wave propagating through the structure is shown in Figure 8a. The generated signal in the low frequency region coincides with signals obtained analytically. The comparison of these signals shows that only the first couple of oscillations coincide and that reflections from the boundaries in FE simulation change the signal completely, increasing the amplitude significantly similar to WebCore panel simulation. This means that for benchmarking sensors for Space vehicles, we have to use long-sided panels just to eliminate reflection.

4. CONCLUSION

This paper discussed several different analyses each of which was designed to model and examine acoustic waves propagating in sandwich panels from the point of using acoustic based methods for SHM. Accordingly, the goal of this work was to analyze systematically elastic wave propagation and scattering in sandwich composite panels and figure out main characteristic features of this propagation in the framework of theoretical 2D and numerical 3D theory of elasticity. It may be concluded that acoustic wave propagation realized during pulsed echo and pitch catch techniques provide an attractive approach for SHM. In order to accomplish the goal of using these techniques for Space Vehicles (detect small-size defects for a minimum set of sensors), extensive experimental and theoretical work should be done in the near future.

NOMENCLATURE

w	transverse displacement
D	bending stiffness
G	Shear stiffness
c	core thickness
t	face sheet thickness
ρ_f	face sheet density
ρ_c	core density
ρ	density per area
r,θ	polar coordinates
ψ_x,ψ_y	rotation about z axis, $\boldsymbol{\psi} = (\psi_x, \psi_y)$.
k	wavenumbers, k_1 k_2 k_3
ε_n	the Neumann factor
ν	Poisson ratio
f	frequency of the PZT excitation
J_n	the Bessel function of the first kind
H_n	the Hankel function of the first kind
a	radius of the hole
r_0	radius of the PZT actuator
$g(t)$	input signal
$G(\omega)$	Fourier transform of the input signal
$H(t)$	the Heaviside function
N	number of oscillations in input signal
n	number of modes used for modeling
h	thickness of the plate

REFERENCES

B.A. Bednarcyk, S.M. Arnold, C.S. Collier, and P.W. Yarrington. (2007). Preliminary Structural Sizing and Alternative Material Trade Study for CEV Crew Module," 48th AIAA/ASME/ASCE/ AHS/ASC Structures, Structural Dynamics, and Materials Conference, Honolulu, HI, April, 2007, pp. 1-32.

B.A. Bednarcyk, S.M. Arnold, and D.A. Hopkins. (2010). Design of Fiber Reinforced Foam Sandwich Panels for Large Ares V Structural Applications. 51st AIAA/ASME /ASCE/ AHS/ ASC Structures, Structural Dynamics, and Materials Conference BR18th 12 - 15 April 2010, Orlando, Florida. 1-19.

R.D. Mindlin. (1951). Influence of rotatory inertia and shear on flexural motions of isotropic, elastic plates, J. Appl. Mech. **18**, 31–38.

P.M. Morse, & H. Feshbach, (1953). Methods of Theore tical. Physics, McGraw-Hill, New York.

Y-H. Pao, C.C. Chao. (1964). Diffractions of flexural waves by a cavity in an elastic plate, AIAA J **2**(11), 2004-2010.

L.R.F. Rose and C.H. Wang (2004). Mindlin plate theory for damage detection: Source solutions. J. Acoust. Soc. Am. **116** (1), 154-171.

D.W. Sleight and D. Paddock, J.Jeans, J. Hudeck. (2008). Structural design and analysis of the upper pressure shell section of a composite crew module. *11th ASCE Aerospace Division International Conference (Earth and Space 2008) Long Beach, CA, USA.*

F. Song, G.L. Huang and K. Hudson. (2009). Guided wave propagation in honeycomb sandwich structures using a piezoelectric actuator/ sensor system. Smart Mater. Struct. vol.18 125007 (8pp).

R. B. Thompson, G. A. Alers, D. O. Thompson, and M. A. Tennison. (1975). Dispersion of flexural elastic waves in honeycomb sandwich panels. J. Acoust. Soc. Am. vol. 57, *No*. 5, 1119-1127.

C. H. Wang, F.K. Chang (2005). Scattering of plate waves by a cylindrical inhomogeneity. Journal of Sound and Vibration, vol. 282, pp. 429-451.

C. H. Wang, J. T. Rose and F.K. Chang. (2004). A synthetic time-reversal imaging method for structural health monitoring. Smart Mater. Struct. 13 , 415-423 .

D. Zenkert. (1997). Ed., The Handbook of Sandwich Construction, EMAS Ltd, Warley, UK.